J. Fluid Mech. (1970), *vol.* 40, *part* 2, *pp.* 343–360
Printed in Great Britain

Self-similar solutions to the second-order incompressible boundary-layer equations

By M. J. WERLE† AND R. T. DAVIS

Engineering Mechanics Department, Virginia Polytechnic Institute, Blacksburg, Virginia

(Received 2 April 1969)

Solutions are obtained for the self-similar form of the incompressible boundary-layer equations for all four second-order contributors, i.e. vorticity interaction, displacement speed, longitudinal and transverse curvature. These results are found to contain all previous self-similar solutions as members of the much larger family of solutions presented here. Numerical solutions are presented for a large number of cases, and several closed form solutions, which may have special significance for the separation problem, are also discussed.

1. Introduction

Although it has long been recognized that approximate solutions of the Navier–Stokes equations obtained via Prandtl's boundary-layer concept represent only the first term of an asymptotic expansion for large Reynolds numbers, it was only within recent history that a consistent higher-order approximation has been formulated by Van Dyke (1962*a*). This was achieved through the recognition that the generalized problem (i.e. solution of the Navier–Stokes equation for high Reynolds number) is one well suited to solution by the formal perturbation techniques employed in numerous other fields of mechanics. Van Dyke's first paper (1962*a*) sets down those equations representing the next level of approximation (termed the second order) above that of Prandtl's equations for two-dimensional or axisymmetric flow of an incompressible fluid, and it is this set of equations with which the present work will deal exclusively.

Reasons for studying the higher-order effects are as varied as the number of investigators who have considered this problem. Aside from the fact that the problem is in itself academically intriguing, work at the second-order level is desperately needed to gain a better insight into the effects of lower Reynolds numbers as they are encountered in high altitude flight and high Mach number wind tunnel tests. Even more basic, though, are questions concerning the nature of the second-order contributions near the point of boundary-layer separation, and of the modifications necessary to classical boundary-layer stability theory due to this new influence. It is hoped that the work contained herein will provide the much-needed vehicle for future work in such studies.

The overall objective of the present work is to conduct a general investigation

† Also, Applied Aerodynamics Division, U.S. Naval Ordnance Laboratory, Silver Spring, Maryland.

of the second-order incompressible boundary-layer equations themselves, in an effort to define the intrinsic characteristics of their solution sets. To this end, analytical and numerical solutions are obtained for a rather general self-similar form of the governing equations for all four second-order contributors, i.e. vorticity interaction, displacement speed, longitudinal curvature, and transverse curvature. As pointed out in Van Dyke's very recent review of higher-order boundary-layer theory (1969), most previously obtained self-similar solutions (see e.g. Narasimha & Ojha 1967, Cooke 1966, or Tani 1954) belong to that class for which the second-order solutions have the same similarity form as that of the first-order solutions (i.e. the Falkner–Skan solutions). The present study removes this restriction and subsequently reveals many significant points necessarily not contained in the more limited earlier studies.† In particular, it is found that the vorticity interaction contribution is always self-similar if the first-order solution is. For the remaining three contributors, displacement speed, longitudinal curvature and transverse curvature, it is found that the solutions are governed by the three parameters respectively representing the second-order pressure gradient, the ratio of longitudinal radius of curvature to the first-order displacement thickness, and the ratio of the transverse curvature to the first-order displacement thickness.

Closed form solutions (in terms of the well documented Falkner–Skan functions) are obtained for a limited range. These include several cases with special significance at the point of first-order separation. In particular, it is found that the displacement speed contribution can proceed through separation with no difficulty for two different second-order pressure gradients. For all other second-order pressure gradients a singularity occurs, thereby indicating that boundary-layer calculations near separation are valid only if proper attention is given to the second-order contributions. Numerical solutions of a large number of cases for the longitudinal and transverse curvature effects well support this same conclusion. These numerical studies also show that the second-order contributors can apparently become singular for any pressure gradient, be it adverse, neutral or favourable, if the second-order parameters take on certain critical values. While the closed form solutions discussed above do support this position, the occurrence of these singularities is apparently without precedent. Even though an attempt is made to interpret the physical significance of these singularities, the full meaning of these phenomena is not at all understood at this time.

2. The boundary-layer equations

Since Van Dyke's original paper (1962*a*) quite clearly sets down the process involved in the formulation of boundary-layer theory to second order, there is no need to rederive the equations here. For reference purposes these will be restated in terms of the stream function ψ and standard surface co-ordinate system (s, n) depicted in figure 1. The non-dimensionalizing scheme is identical to that of

† The authors wish to thank Van Dyke for pointing out that special cases of this more general class of solutions was considered earlier by both Seban & Bond (1951) and Kuo (1953).

Van Dyke (1962*a*), with velocities referenced to the free-stream velocity U_∞, pressures reference to the dynamic pressure ρU_∞^2, and the Reynolds number defined as

$$R = \frac{\rho U_\infty L}{\mu} = \frac{1}{\epsilon^2}, \tag{1}$$

μ being the viscosity and L a reference length (frequently taken as $(1/\kappa)_{s=0}$, κ being the surface longitudinal curvature). It should be noted that since only similar flows are to be considered here, the choice of a reference length is of no consequence to the final results. Further recall that basic to the present study are the assumptions of constant fluid properties (ρ and μ) and a uniform mainstream (U_∞) aside from possible external shear.

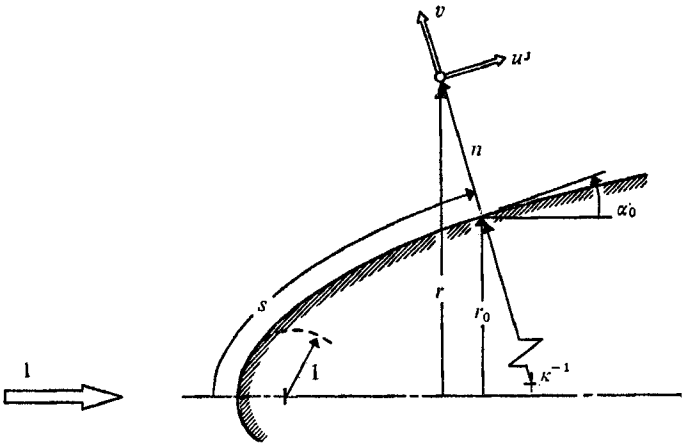

FIGURE 1. Non-dimensional co-ordinates for boundary layer.

Asymptotic expansions are now formed for the inviscid stream function

$$\psi_i(s, n; \epsilon) \sim \Psi_1(s, n) + \epsilon\Psi_2(s, n) + \ldots, \tag{2}$$

the s component of velocity

$$u_i(s, n; \epsilon) \sim U_1(s, n) + \epsilon U_2(s, n) + \ldots, \tag{3}$$

the n component of velocity

$$v_i(s, n; \epsilon) \sim V_1(s, n) + \epsilon V_2(s, n) + \ldots, \tag{4}$$

and the pressure

$$p_i(s, n; \epsilon) \sim P_1(s, n) + \epsilon P_2(s, n) + \ldots. \tag{5}$$

Use is also to be made of the Bernoulli function defined as

$$B_1(\Psi_1) = P_1 + \tfrac{1}{2}(U_1^2 + V_1^2). \tag{6}$$

These expansions are found to be invalid near the wall ($n = 0$), and subsequently inner expansions are formed by first stretching the normal co-ordinate to obtain the inner variable,

$$N = n/\epsilon. \tag{7}$$

The assumed inner (viscous) expansions are

$$\psi_v(s,n;\epsilon) \sim \epsilon\psi_1(s,N)+\epsilon^2\psi_2(s,N)+\ldots, \tag{8}$$

$$u_v(s,n;\epsilon) \sim u_1(s,N)+\epsilon u_2(s,N)+\ldots, \tag{9}$$

and

$$v_v(s,n;\epsilon) \sim \epsilon v_1(s,N)+\epsilon^2 v_2(s,N)+\ldots, \tag{10}$$

where

$$u_1 = \frac{1}{r_0^j}\frac{\partial\psi_1}{\partial N}, \quad v_1 = -\frac{1}{r_0^j}\frac{\partial\psi_1}{\partial s}; \tag{11}$$

and

$$u_2+\left(\frac{j\cos\alpha_0}{r_0}\right)Nu_1 = \frac{1}{r_0^j}\frac{\partial\psi_2}{\partial N},$$

$$v_2+\left(\kappa+\frac{j\cos\alpha_0}{r_0}\right)Nv_1 = -\frac{1}{r_0^j}\frac{\partial\psi_2}{\partial s}, \tag{12}$$

where r_0 and α_0 are defined in figure 1, and $j = 0$ for two-dimensional flows, $j = 1$ for the axisymmetric case. With these definitions, the governing equations and their corresponding boundary conditions are written as:

first-order,

$$\psi_{1_{NNN}}+\left(\psi_{1_s}\frac{\partial}{\partial N}-\psi_{1_N}\frac{\partial}{\partial s}\right)r_0^{-j}\psi_{1_N} = -r_0^j U_1(s,0)\,U_{1_s}(s,0), \tag{13}$$

with

$$\psi_1(s,0) = \psi_{1_N}(s,0) = 0, \tag{14}$$

and

$$\psi_{1_N}(s,\infty) = r_0^j U_1(s,0); \tag{15}$$

second-order,

$$\begin{aligned}\psi_{2_{NNN}}&+\left(\psi_{1_s}\frac{\partial}{\partial N}-\psi_{1_N}\frac{\partial}{\partial s}\right)r_0^{-j}\psi_{2_N}+\left(\psi_{2_s}\frac{\partial}{\partial N}-\psi_{2_N}\frac{\partial}{\partial s}\right)r_0^{-j}\psi_{1_N}\\ &= r_0^j\frac{\partial}{\partial s}\kappa\left[NU_1^2(s,0)+\int_N^\infty\{U_1^2(s,0)-r_0^{-2j}\psi_{1_N}^2\}\,dN\right]\\ &\quad-\kappa[N\psi_{1_{NNN}}+\psi_{1_{NN}}+r_0^{-j}\psi_{1_s}\psi_{1_N}]-r_0^jB_1'(0)\frac{d}{ds}(r_0^jU_1(s,0)\,\delta_1^*)\\ &\quad-r_0^j\frac{d}{ds}[U_1(s,0)\,U_2(s,0)]+\frac{j\cos\alpha_0}{r_0}\left[\psi_{1_{NN}}+\left(\psi_{1_s}\frac{\partial}{\partial N}-\psi_{1_N}\frac{\partial}{\partial s}\right)N\psi_{1_N}\right.\\ &\quad\left.-Nr_0^jU_1(s,0)\,U_{1_s}(s,0)\right],\end{aligned} \tag{16}$$

with

$$\psi_2(s,0) = \psi_{2_N}(s,0) = 0, \tag{17}$$

and

$$\psi_{2_N}(s,N)\to Nr_0^j\left[\left(\frac{j\cos\alpha_0}{r_0}-\kappa\right)U_1(s,0)+r_0^jB_1'(0)\right] \quad \text{as} \quad N\to\infty. \tag{18}$$

Since the second-order problem is linear, further study of (16) will employ its subdivision into those four components appearing explicitly in the problem (as first suggested by Rott & Lenard 1959). These components represent direct contributions due to external vorticity (ψ_2^v), displacement speed (ψ_2^d), longitudinal curvature (ψ_2^L), and transverse curvature (ψ_2^T), leading to the redefinition of the second-order stream function as

$$\psi_2 = B_1'(0)\,\psi_2^v+U_2(s,0)\,\psi_2^d+\kappa\psi_2^L+\frac{j\cos\alpha_0}{r_0}\psi_2^T. \tag{19}$$

3. The self-similar equations

Formulation of the self-similar boundary-layer problem is faced with the immediate difficulty of choosing a co-ordinate system in which to work. Kaplun's (1954) study of the effects of co-ordinate choice on the boundary-layer approximations clearly shows that an optimal system can be formulated for the first-order boundary-layer problem, but, as pointed out by Van Dyke (1964), the rules for finding such at higher-order levels are not yet known. The formulation employed here will make use of one of the more standard sets of dependent variables. Görtler's (1957) variables are one of the more attractive available, since they produce a rather compact form for both the two-dimensional and axisymmetric boundary-layer equations, and further may be easily generalized to the compressible problem via the Levy–Lees definitions (see Lees 1956). Thus, for the present study, the dependent variables will be taken as†

$$\xi = \int_0^s U_1 r_0^{2j}\, ds \quad \text{and} \quad \eta = \frac{U_1 r_0^j}{\sqrt{(2\xi)}} N. \tag{20}$$

Introduction of the above transformation, along with further change of the dependent variable to its usual similarity form,

$$\psi_1 = \sqrt{(2\xi)} f(\eta), \tag{21}$$

produces the familiar Falkner–Skan equation

$$f''' + f f'' + \beta(1 - f'^2) = 0, \tag{22}$$

where

$$\beta = \frac{2\xi}{U_1}\frac{dU_1}{d\xi}. \tag{23}$$

A rather general form (which excludes the classical internal flows) of the self-similar second-order equations is obtained by defining the respective stream functions as

vorticity,
$$\psi_2^v = \frac{2\xi}{U_1^2} g_1(\eta), \tag{24}$$

displacement speed,
$$\psi_2^d = \frac{\sqrt{(2\xi)}}{U_1} g_2(\eta) \tag{25}$$

longitudinal curvature,
$$\psi_2^L = \frac{2\xi}{r_0^j U_1} g_3(\eta), \tag{26}$$

transverse curvature,
$$\psi_2^T = \frac{2\xi}{r_0^j U_1} g_4(\eta). \tag{27}$$

Further definition of the operator L as

$$L \equiv \frac{d^3}{d\eta^3} + f\frac{d^2}{d\eta^2} - a_j f'\frac{d}{d\eta} + b_j f'', \quad (j = 1, \ldots, 4) \tag{28}$$

† In the interest of eliminating repetition, the inviscid properties evaluated at $n = 0$ (for example, $U_1(s, 0)$ or $U_2(s, 0)$) will henceforth be written without their arguments (for example, U_1 or U_2).

allows the four second-order problems to be written as

$$Lg_j = G_j, \tag{29}$$

with the boundary conditions specified as

$$g_j(0) = g_j'(0) = 0 \tag{30}$$

and

$$g_j'(\eta) \to F_j(\eta) \quad \text{as} \quad \eta \to \infty. \tag{31}$$

The appropriate a_j, b_j, G_j and F_j are given in table 1 with the definition of all terms involved. It is seen that in this form the problem is ideally suited to the numerical solution of the governing equations as is required in general.†

j	Definitions	a_j	b_j	F_j	G_j
1	External vorticity	1	$2(1-\beta)$	η	$-\Delta_1$
2	Displacement speed $\pi_2 = \dfrac{2\xi}{U_2}\dfrac{dU_2}{d\xi}$	$\pi_2+\beta$	$1+\pi_2-\beta$	1	$-(\pi_2+\beta)$
3	Longitudinal curvature $\pi_3 = \dfrac{2\xi}{\kappa/r_0^j}\dfrac{d(\kappa/r_0^j)}{d\xi}$	$1+\pi_3+\beta$	$2+\pi_3-\beta$	$-\eta$	$\eta\left[\beta\left(1+\dfrac{\pi_3}{1+\beta}\right)-f'''\right] + \dfrac{\pi_3}{1+\beta}[f''+ff'] + \left(1+\dfrac{\pi_3}{1+\beta}\right)\Delta_1$
4	Transverse curvature $\pi_4 = \dfrac{2\xi}{\cos\alpha_0/r_0^{2j}}\dfrac{d(\cos\alpha_0/r_0^{2j})}{d\xi}$	$1+\pi_4+\beta$	$2+\pi_4-\beta$	η	$\eta[ff''-(1+\pi_4)f'^2 -\beta]+f''+ff'$

TABLE 1. Definitions for self-similar second-order boundary layers.

4. The boundary-layer functions

A straightforward application of the functional definitions given in (21) and (24) through (27) to the shear stress and displacement thickness definitions (see Werle & Davis (1966) for the proper definition of δ^* to second order) results in the following expressions:

shear stress,

$$\tau_w = \epsilon^2\left(\frac{\partial u_v}{\partial n}\right)_{n=0} \sim \epsilon\frac{r_0^j U_1^2}{\sqrt{(2\xi)}}f''(0) + \epsilon^2\left[\frac{r_0^j U_1^2}{\sqrt{(2\xi)}}\frac{U_2}{U_1}g_2''(0) + r_0^j B_1' g_1''(0) + \kappa U_1 g_3''(0) + \frac{j\cos\alpha_0}{r_0}U_1 g_4''(0)\right] \tag{32}$$

† Using the self-similar form of the first-order displacement thickness, it may be shown that the longitudinal curvature problem can be stated entirely in terms of the product $\kappa\delta_1^*$, instead of the parameter π_3, and that the transverse curvature problem can be stated in terms of $\delta_1^*\cos\alpha_0/r_0^j$ instead of π_4. While such a formulation might appear more compact, the present studies will be conducted in terms of the π_j, so that curvature and pressure gradient effects may be considered independently.

and displacement thickness,

$$\delta^* \sim \epsilon \frac{\sqrt{(2\xi)}}{r_0^j U_1} \Delta_1 + \epsilon^2 \left[\frac{\sqrt{(2\xi)}}{r_0^j U_1} \frac{U_2}{U_1} \Delta_2^d + \frac{2\xi}{r_0^{2j} U_1^2} \left(\frac{r_0^j B_1'}{U_1} \Delta_2^v - \kappa \Delta_2^L + \frac{j \cos \alpha_0}{r_0} \Delta_2^T \right) \right], \quad (33)$$

where the following definitions have been applied throughout

$$\Delta_1 = \lim_{\eta \to \infty} (\eta - f), \quad (34a)$$

$$\Delta_2^v = \lim_{\eta \to \infty} (\tfrac{1}{2}\eta^2 - g_1) - \tfrac{1}{2}\Delta_1^2, \quad (34b)$$

$$\Delta_2^d = \lim_{\eta \to \infty} (\eta - g_2) - \Delta_1, \quad (34c)$$

$$\Delta_2^L = \lim_{\eta \to \infty} (\tfrac{1}{2}\eta^2 + g_3) - \tfrac{1}{2}\Delta_1^2, \quad (34d)$$

$$\Delta_2^T = \lim_{\eta \to \infty} (\tfrac{1}{2}\eta^2 - g_4) - \tfrac{1}{2}\Delta_1^2. \quad (34e)$$

A consistent definition of the momentum thickness to second order has been proposed by Werle & Davis (1966) and evaluated by Werle (1968).

5. Exact relations for the second-order equations

Since, in general, the solutions of the similarity equations given in (29) and table 1 must be obtained by numerical integration techniques, it is apparent that any exact relations which might be obtained would be quite useful.

Considering the displacement speed equations, it is found that two sets of solutions may be written in terms of the first-order function f, for specific distribution of π_2 as a function of β. The first of these is for the case of $\pi_2 = \beta$, for which the governing equation becomes

$$g_2''' + f g_2'' - 2\beta f' g_2' + f'' g_2 = -2\beta. \quad (35)$$

It is easily verified that the solution of this equation for any β is given by

$$g_2 = \tfrac{1}{2}(\eta f' + f). \quad (36)$$

This result was previously given by Van Dyke (1962*b*) for the specific cases of $\beta = \frac{1}{2}$ and 1 (corresponding to flows at axisymmetric and planar stagnation points respectively) and by Kuo (1953) for $\beta = 0$ (corresponding to flow over a cusped leading edge). The present investigation indicates the result holds for any β so long as $\pi_2 = \beta$. In particular, it implies that if $\pi_2 = \beta_{\text{sep}} = -0{\cdot}198838$, i.e. the first-order boundary is at its separation point, then the second-order boundary layer is perfectly well behaved, and in fact the shear due to displacement speed, as given by

$$g_2''(0) = \tfrac{3}{2} f''(0), \quad (37)$$

is also zero.

A second set of exact solutions may be obtained for that class of flows for which

$$\pi_2 = 2(\beta - 1), \quad (38)$$

but

$$\beta \neq 0, \quad (39)$$

for which the governing equation reduces to

$$g_2''' + fg_2'' + (2-3\beta)f'g_2' - (1-\beta)f''g_2 = (2-3\beta), \tag{40}$$

and its solution is given by

$$g_2 = (1/\beta)\,[(\beta-1)\,\eta f' + f]. \tag{41}$$

This result includes that found by Van Dyke (1962*b*) for the flow in the leading edge region of a blunt body with asymmetry, which is reproduced by (41) for $\beta = 1$.

The solution given by (41) is of interest for two specific reasons. First, it is seen that the shear stress for this case, given by

$$g_2''(0) = \frac{2\beta-1}{\beta} f''(0), \tag{42}$$

suffers an infinite discontinuity across $\beta = 0$, for which case $\pi_2 = -2$. The physical significance of this result is not at all understood, but it is precisely the type of result which later will be found to occur in the numerical analysis for all π_2 at some specific β.

A second interesting point, concerning the solution given by (41), is the behaviour of the solution near separation (i.e. $\beta = -0{\cdot}198838$). As shown by (42), the shear stress vanishes at this point and, again, it is seen that one can arrive at separation without the second-order effects causing any new difficulty.

6. Numerical solutions of the similarity equations

The solutions of the second-order similarity equations (see (29) and table 1) have been obtained by numerical integration for a wide range of β and the π_j's.† These solutions were obtained on an IBM 7094 computer using a single precision fourth-order Runge–Kutta scheme with a constant step size of $\Delta\eta = 0{\cdot}05$ throughout.‡ The necessary numerical solutions to the Falkner–Skan equation were obtained using Smith's (1954) values of $f''(0)$ to start the integration.

As previously mentioned, the vorticity problem introduces no new parameters and, thus, these solutions may be tabulated once and for all for any β of interest. Table 2 presents such a listing of the second-order shear and displacement thickness for all available values of β. These results are also presented graphically in figures 2 (*a*) and (*b*), along with typical velocity profiles in figure 3. Each of these figures shows clearly that the direct contribution of vorticity to the second-order boundary layer is quite small in the presence of strong favourable pressure gradients but becomes increasingly significant as separation is approached. The singular nature of the results near separation is a clear indication the first-order solutions are no longer valid in this region, since the second-order effects apparently grow to first-order size. Figure 4 shows that near separation this singularity is approached according to

$$g_1''(0) \propto (\beta - \beta_{\text{sep}})^{-0{\cdot}46}. \tag{43}$$

† All of the numerical results presented graphically in this paper are presented in tabular form by Werle (1968).

‡ In general, calculations near $\beta = 2$ required double precision arithmetic to produce meaningful second-order displacement and momentum thickness.

Numerical solutions to the displacement speed problem are presented in figures 5(*a*) and (*b*) for the full range of $-2{\cdot}5 \leqslant \pi_2 \leqslant 2{\cdot}0$. These results have been verified directly through comparison with the 'exact' solutions discussed above (these cases are pointed out in figure 5 when appropriate).

β	$g_1''(0)$	Δ_2^g
2·0	1·1106	−0·0279
1·6	1·1979	−0·1582
1·2	1·3214	−0·3086
1·0	1·4065†	−0·4252
0·8	1·5172	−0·5919
0·6	1·6688	−0·8447
0·5	1·7686†	−1·0255
0·4	1·8930	−1·2656
0·3	2·0537	−1·5979
0·2	2·2720	−2·0860
0·1	2·5918	−2·8697
0·05	2·8191	−3·4709
0·04	2·8729	−3·6180
0·03	2·9300	−3·7763
0·02	2·9909	−3·9474
0·01	3·0561	−4·1328
0·008	3·0697	−4·1717
0·006	3·0834	−4·2114
0·004	3·0974	−4·2517
0·002	3·1116	−4·2927
0·001	3·1188	−4·3137
0	3·1260‡	−4·3344
−0·05	3·5729	−5·6865
−0·10	4·3154	−8·1414
−0·14	5·4795	−12·3960
−0·16	6·6329	−16·9689
−0·18	9·2569	−28·2142
−0·19	13·1530	−46·0875
−0·195	19·4652	−76·3405
−0·198838	∞	−∞

† Originally given by Van Dyke (1962*b*).
‡ Originally given by Murray (1961).

TABLE 2. Vorticity interaction solutions.

Considering e.g. the shear stress distributions of figure 5(*a*), it is seen that the first-order separation point evidently represents a singularity in the second-order quantities for all but two values of π_2 corresponding to $\pi_2 = -0{\cdot}198838$ and $\pi_2 = -2{\cdot}397676$, a result implied by the 'exact' solutions given in (37) and (42), respectively. Since (32) gives the displacement speed contribution to the shear stress as

$$\tau_{2_w}^d = \frac{r_0^j U_1^2}{\sqrt{(2\xi)}} \frac{U_2}{U_1} g_2''(0), \tag{44}$$

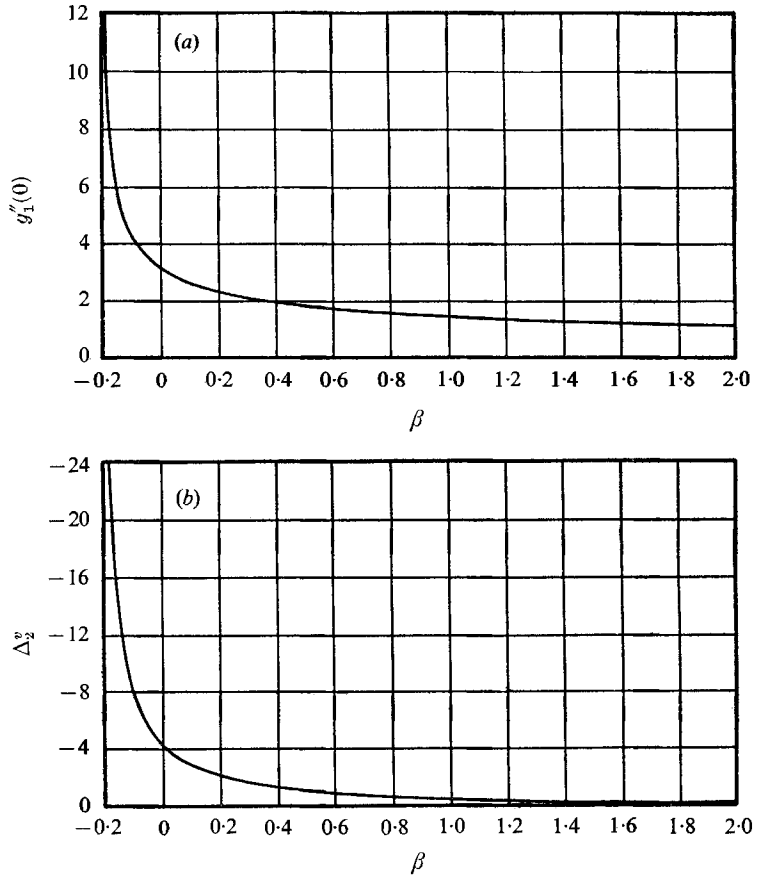

FIGURE 2. Vorticity interaction solutions: (*a*) shear stress, (*b*) displacement thickness.

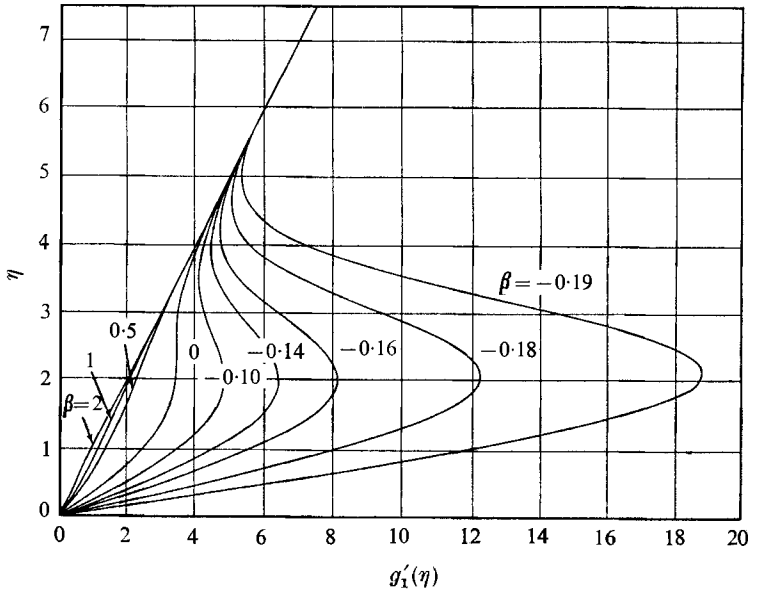

FIGURE 3. Vorticity interaction solutions: velocity profiles.

for these two special cases one could seemingly arrive at the separation point with zero second-order shear so that the ordering scheme (in Reynolds number) would be preserved. For those solutions with singularities only at $\beta = \beta_{\text{sep}}$, it has been found that, as in the vorticity interaction problem, the second-order shear stress apparently approaches the limit variation of (43).

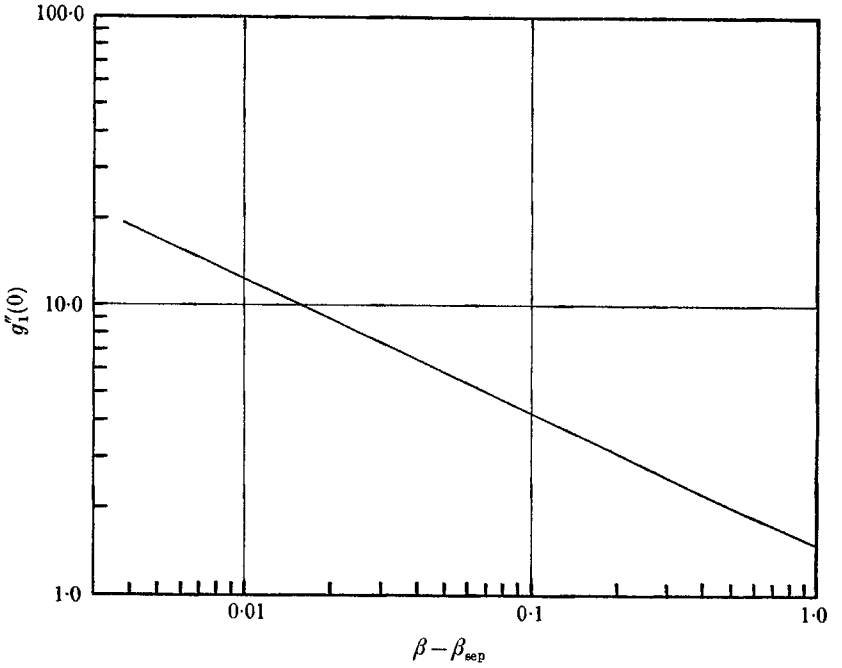

FIGURE 4. Vorticity interaction solutions: shear stress variation near $\beta = \beta_{sep}$.

Another rather interesting (and equally surprising) result of this present study was the appearance of singularities in all the second-order functions for $\pi_2 < 0$ at $\beta > \beta_{\text{sep}}$ (see e.g. figure 5(*a*), $\pi_2 = -2$). The occurrence of such is not unprecedented since (42) has already served notice that this would occur at $\beta = 0$, $\pi_2 = -2$. A simple trial and error iterative scheme has been used better to locate the singularities, and the resulting variation of the critical value of π_2 is given in table 3 and figure 6. Note that it can be shown that the second-order pressure gradient is proportional to $(\beta + \pi_2) U_2/U_1$, so that, if near $\pi_{2_{\text{crit}}}(\beta + \pi_2 \approx -2$ according to table 3) $U_2 > 0$, then there exists a relatively strong adverse pressure gradient. For this case, (44) gives $\tau_{2_w}^d < 0$, which presumably indicates an early separation point,† as might be expected. On the other hand, the case of $U_2 < 0$ produces rather confusing results, for here the second-order pressure gradient is favourable, and $\tau_{2_w}^d > 0$ indicates delay of separation. The occurrence of the singularities then implies a breakdown in the boundary-layer assumptions not necessarily associated with separation, and as yet completely unexplainable.

† Note that, near the critical values, $g_2''(0)$ is generally negative.

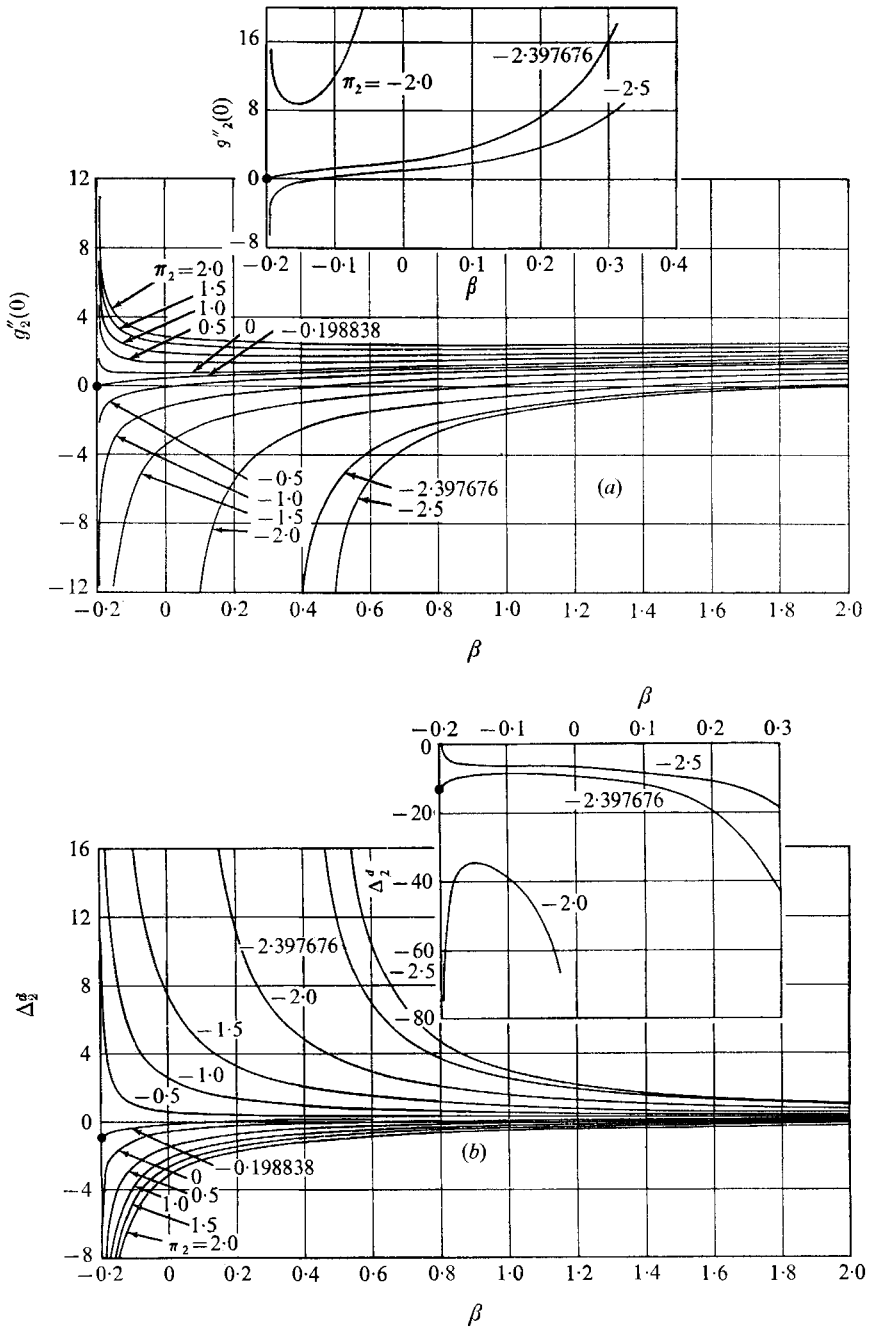

FIGURE 5. Displacement speed solutions: (*a*) shear stress, (*b*) displacement thickness. ● → exact solutions of § 5.

Numerical solutions to the longitudinal curvature problem have been obtained for all available β and π_3 ranging from 2·0 to $-3{\cdot}5$. The results of these studies are given in figures 7(*a*) and (*b*). As for the displacement speed problem, it is seen that the contribution is at a minimum for a strong positive pressure gradient and grows progressively larger as separation is approached. Here also it is found that a singularity occurs at separation for all but two values of π_3, given approximately as $-1{\cdot}5 < \pi_3 < -1{\cdot}0$ and $-3{\cdot}5 < \pi_3 < -3{\cdot}0$, possibly indicating the existence of well behaved boundary layers right up to separation. Again, it was found that those solutions with singularities only at $\beta = \beta_{sep}$ closely follow the relation given in (43).

β	π_{2crit}	$\pi_{2crit} + \beta$
2·0	−4·134	−2·134
1·6	−3·729	−2·129
1·2	−3·323	−2·123
1·0	−3·118	−2·118
0·5	−2·592	−2·092
0·2	−2·254	−2·054
0·1	−2·133	−2·033
0	−2·000	−2·000
−0·1	−1·845	−1·945
−0·16	−1·719	−1·879
−0·18	−1·659	−1·839
−0·19	−1·616	−1·806
−0·195	−1·585	−1·780

TABLE 3. Critical values of second-order parameters.

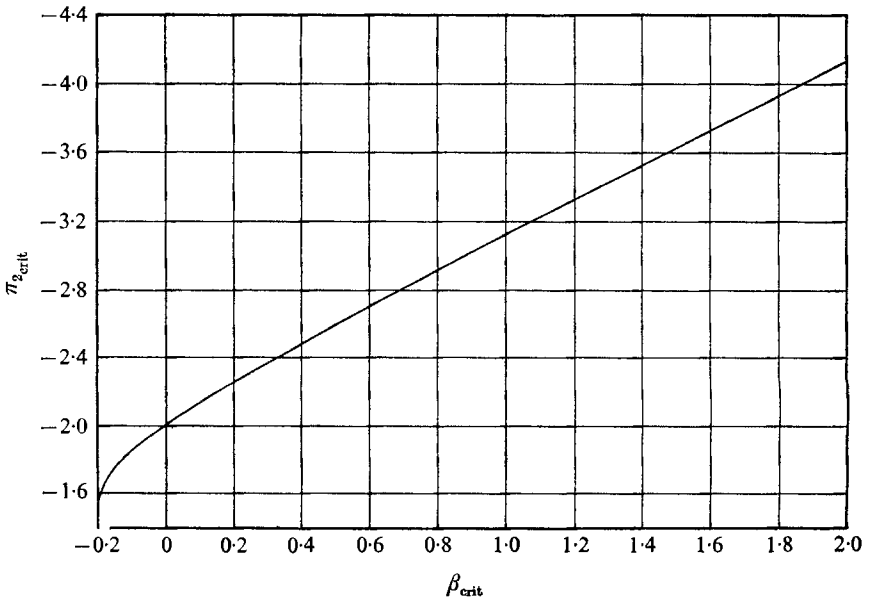

FIGURE 6. Critical parameter values for the displacement speed problem.

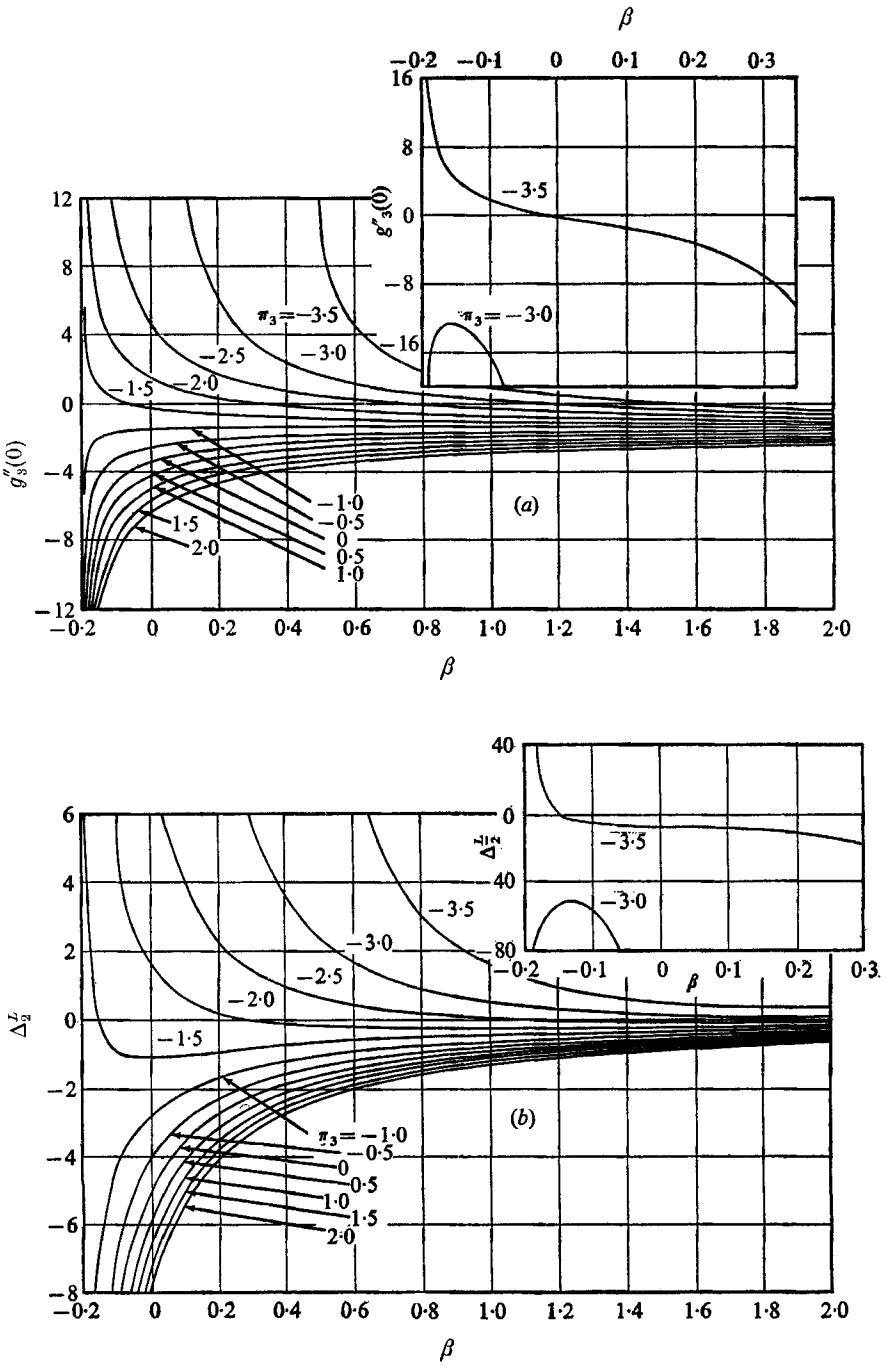

FIGURE 7. Longitudinal curvature solutions: (*a*) shear stress, (*b*) displacement thickness.

Quite naturally, the present solutions imply that the second-order equations are very sensitive to the rate of change of curvature (note from table 1 that π_3 is essentially a measure of the rate of change of curvature). Carrying this idea one step further, one may consider the case of $\pi_3 = 0$ (i.e. $\kappa =$ constant as on a cusped leading edge or a cylinder); for the concave case, the shear stress contribution, given in (32) as

$$\tau_{2_w}^L = \kappa U_1 g_3''(0), \tag{45}$$

is positive, thereby indicating a delay in separation. The convex case ($\kappa > 0$) of course experiences a decrease in shear, and thus predicts an earlier separation as would be expected. Further, if $\pi_3 > 0$ (roughly corresponding to the indicated geometries of figure 8), then convex curvature experiences even earlier separation (since at a given β, $g_3''(0)$ is larger negative for $\pi_3 > 0$ than for $\pi_3 = 0$), while the case of $\pi_3 < 0$ experiences a further delay of separation over that for $\pi_3 = 0$.†

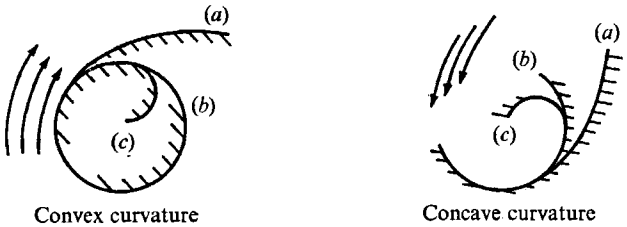

FIGURE 8. Flow geometries indicative of constant π_3: (*a*) $\pi_3 < 0$, (*b*) $\pi_3 = 0$, (*c*) $\pi_3 > 0$.

Most interesting are the results predicted for $\pi_3 \ll 0$, corresponding to a region of relatively rapid decrease in curvature ($\pi_3 = -\infty$ would be roughly equivalent to a line tangent to the circle depicted in figure 8). The appearance of singularities at $\beta > \beta_{\text{sep}}$ for these cases evidently lends some credence to the suspicion that the boundary-layer equations are invalid in regions of discontinuous body curvature.

For the sake of completeness, trial and error studies were conducted to define the locations of the above mentioned singularities, and it was found that, within the accuracy of the solution, the critical values of π_3 are given by

$$\pi_{3_{\text{crit}}} = \pi_{2_{\text{crit}}} - 1. \tag{46}$$

Figures 9(*a*) and (*b*) present solutions of the transverse curvature equation for all available β and π_4 ranging from $-3{\cdot}5$ to $2{\cdot}0$. Due to the similarity of the longitudinal and transverse curvature equations (see table 1), it is not surprising to find the essential features of the solutions very nearly the same (compare $-g_3''(0)$ of figure 7 with $g_4''(0)$ of figure 9). Here again it is found that the second-order contribution is at a minimum for strong favourable pressure gradients and grows progressively larger as separation is approached. There evidently exists but one single value of π_4, however, for which the separation point does not represent a singularity, and this occurs between $\pi_4 = -1{\cdot}5$ and $-2{\cdot}0$. Again

† Both these results would, of course, be reversed for the concave curvature case.

one is led to the conclusion that for this value of π_4 the boundary-layer assumptions would remain valid throughout the separation process, while all remaining cases approach separation according to the now familiar relation

$$g_4''(0) \propto (\beta - \beta_{sep})^{-0.46}. \tag{47}$$

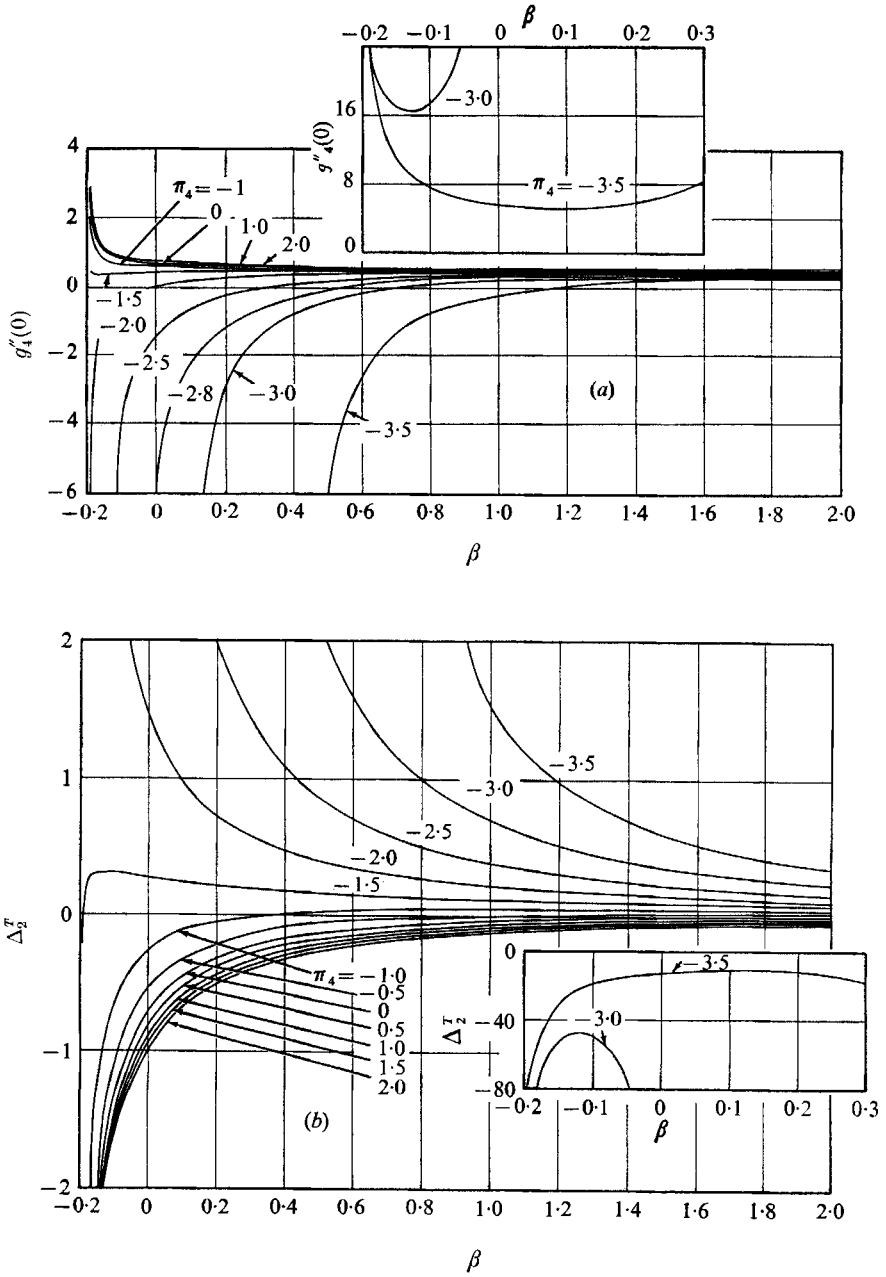

FIGURE 9. Transverse curvature solutions: (*a*) shear stress, (*b*) displacement thickness.

Further review of figures 9(*a*) and (*b*) clearly indicates the existence of singularities quite similar to those occurring for the displacement speed and curvature problems. Trial and error solutions were employed to better locate the critical π_4, and it was found that to within three decimal places

$$\pi_{4_{\text{crit}}} = \pi_{2_{\text{crit}}} - 1, \tag{48}$$

with $\pi_{2_{\text{crit}}}$ given in table 3. The physical significance of these singularities is explainable, on a limited scale, through consideration of the series of typical axisymmetric flow geometries depicted in figure 10. For all these flows $\cos\alpha_0/r_0 > 0$, so that the shear stress (see (32)) has the same sign as $g_4''(0)$. Comparing figure 10 and the shear stress distributions of figure 9(*a*), it is evident that, as one moves from $\pi_4 > 0$ (case (*a*) of figure 10) to $\pi_4 < 0$ (case (*c*)), the shear stress becomes less positive, indicating that the transverse curvature effect is becoming less effective in delaying separation. Finally, though, as π_4 becomes $\ll 0$ (case (*d*)), the second-order contribution actually begins to promote earlier separation (when $g_4''(0)$ becomes < 0). Evidently the appearance of the singularities for $\beta > \beta_{\text{sep}}$ signals the breakdown of the boundary-layer equations for regions in which the transverse curvature changes rapidly.

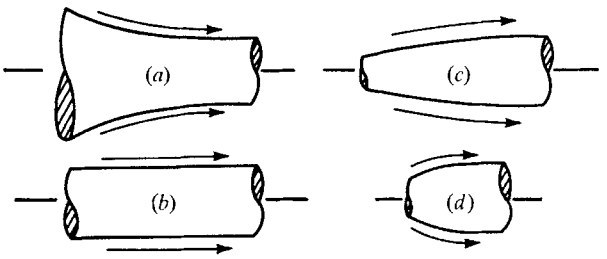

FIGURE 10. Flow geometries indicative of constant π_4:
(*a*) $\pi_4 > 0$, (*b*) $\pi_4 = 0$, (*c*) $\pi_4 < 0$, (*d*) $\pi_4 \ll 0$.

7. Discussion of results

The preceding sections have sought to give some insight into the characteristics of higher-order boundary-layer theory through study of the appropriate self-similar form of the governing equation. The major contribution of the present study is perhaps that it allows some insight into the nature of the governing equations themselves.

It was interesting to find that, while in general the approach to separation caused singularities to appear in the second-order contributions, there were isolated cases in which this did not occur. The appearance of singularities near separation was not at all surprising, since it lends some support to the growing belief that the boundary-layer equations themselves are not valid in this region. More intriguing, though, is the fact that both the exact solutions and the numerical studies show clearly that certain combinations of parameters will allow separation to be approached with no difficulty, and that for these cases the second-order shear vanishes completely. This result lends strong support to the discovery of Catherall & Mangler (1966) that the appearance of the

singularity in the first-order equations near separation may well be unrealistic, and due solely to the misrepresentation of the true pressure gradient in this region. The present self-similar solutions clearly imply that, under certain conditions, the point of zero shear (now to second-order, since the respective $g_j''(0)$ vanish) can be attained with no new difficulty introduced by the second-order contributors. The full significance of this result is not completely understood at the present time, but certainly it indicates one area in which further research could well prove fruitful.

By far the most surprising aspect of the self-similar solutions generated here was the appearance of singularities in all the second-order quantities prior to first-order separation. To the authors' knowledge, there is no precedent for this result, and only a limited rationale for its occurrence can be given at this time. As was indicated, these singularities appear in regions of large negative π_j, corresponding to regions of rapid change in either longitudinal or transverse curvature, and to regions of large second-order pressure gradients. The presence of the singularities certainly indicates that the self-similar results are no longer of second order, but it is not yet clear how to relate their occurrence to physical situations.

REFERENCES

CATHERALL, D. & MANGLER, K. W. 1966 *J. Fluid Mech.* **26**, 163–82.

COOKE, J. C. 1966 *RAE Tech. Rep.* 66044.

GÖRTLER, H. 1957 *J. Math. Mech.* **6**, 1–66.

KAPLUN, S. 1954 *ZAMP* **5**, 111–35.

KUO, Y. H. 1953 *J. Math. Phys.* **32**, 83–101.

LEES, L. 1956 *Jet Propul.* **26**, 259–69.

MURRAY, J. D. 1961 *J. Fluid Mech.* **11**, 309–16.

NARASIMHA, R. & OJHA, S. K. 1967 *J. Fluid Mech.* **29**, 187–99.

ROTT, N. & LENARD, M. 1959 *J. Aero. Sci.* **26**, 542–43.

SEBAN, R. A. & BOND, R. 1951 *J. Aero. Sci.* **18**, 671–5.

SMITH, A. M. O. 1954 IAS Fairchild Fund Preprint FF-10.

TANI, I. 1954 *J. Japan Soc. Mech. Engrs.* **54**, 596–8.

VAN DYKE, M. 1962*a* *J. Fluid Mech.* **14**, 161–77.

VAN DYKE, M. 1962*b* *J. Fluid Mech.* **14**, 481–95.

VAN DYKE, M. 1964 *Perturbation Methods in Fluid Mechanics*. New York: Academic Press.

VAN DYKE, M. 1969 *Annual Review of Fluid Mechanics*, vol. 1. New York: Annual Reviews Inc.

WERLE, M. J. 1968 U.S. Naval Ordnance Laboratory TR 68-19.

WERLE, M. J. & DAVIS, R. T. 1966 *Int. J. Engr. Sci.* **4**, 423–31.